Report

Cell Reports

mGluR-LTD at Excitatory and Inhibitory Synapses in the Lateral Habenula Tunes Neuronal Output

Graphical Abstract

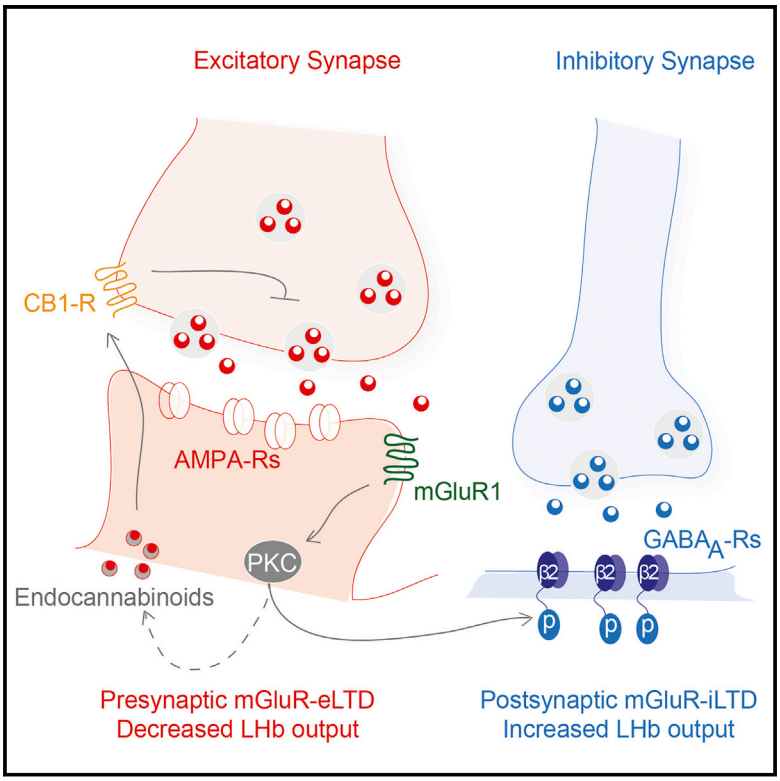

Authors

Kristina Valentinova, Manuel Mameli

Correspondence

manuel.mameli@inserm.fr

In Brief

Valentinova and Mameli show that mGluR1s in the lateral habenula (LHb) triggers PKC-dependent depression of excitatory and inhibitory transmission, allowing for bidirectional tuning of neuronal output via distinct presynaptic and postsynaptic mechanisms.

Highlights

- mGluR1 induces LTD of excitatory and inhibitory transmission in the LHb
- PKC mediates the induction of mGluR-LTD in the LHb
- Divergent expression mechanisms underlie mGluR-eLTD and -iLTD
- mGluR-eLTD and -iLTD decide the direction of LHb neuronal output

Valentinova & Mameli, 2016, Cell Reports *16*, 2298–2307
August 30, 2016
http://dx.doi.org/10.1016/j.celrep.2016.07.064

OPEN ACCESS
CellPress

Cell Reports
Report

mGluR-LTD at Excitatory and Inhibitory Synapses in the Lateral Habenula Tunes Neuronal Output

Kristina Valentinova[1,2,3] and Manuel Mameli[1,2,3,4,*]
[1]Institut du Fer à Moulin, 75005 Paris, France
[2]Inserm, UMR-S 839, 75005 Paris, France
[3]Université Pierre et Marie Curie, 75005 Paris, France
[4]Lead Contact
*Correspondence: manuel.mameli@inserm.fr
http://dx.doi.org/10.1016/j.celrep.2016.07.064

SUMMARY

Excitatory and inhibitory transmission onto lateral habenula (LHb) neurons is instrumental for the expression of positive and negative motivational states. However, insights into the molecular mechanisms modulating synaptic transmission and the repercussions for neuronal activity within the LHb remain elusive. Here, we report that, in mice, activation of group I metabotropic glutamate receptors triggers long-term depression at excitatory (eLTD) and inhibitory (iLTD) synapses in the LHb. mGluR-eLTD and iLTD rely on mGluR1 and PKC signaling. However, mGluR-dependent adaptations of excitatory and inhibitory synaptic transmission differ in their expression mechanisms. mGluR-eLTD occurs via an endocannabinoid receptor-dependent decrease in glutamate release. Conversely, mGluR-iLTD occurs postsynaptically through PKC-dependent reduction of β2-containing $GABA_A$-R function. Finally, mGluR-dependent plasticity of excitation or inhibition decides the direction of neuronal firing, providing a synaptic mechanism to bidirectionally control LHb output. We propose mGluR-LTD as a cellular substrate that underlies LHb-dependent encoding of opposing motivational states.

INTRODUCTION

Excitatory and inhibitory projections onto the lateral habenula (LHb) control the direction of neuronal output, contributing to the encoding of rewarding and aversive stimuli (Shabel et al., 2012, 2014; Stamatakis et al., 2013). Moreover, in rodent models of addiction and depression, glutamatergic and GABAergic synaptic plasticity modulates LHb neuronal firing, which is in turn instrumental for depression-like phenotypes (Lecca et al., 2016; Maroteaux and Mameli, 2012; Meye et al., 2015; Shabel et al., 2014). This highlights the behavioral relevance of synaptic adaptations in the LHb, heightening the need of understanding its underlying cellular processes.

Group I metabotropic glutamate receptor (mGluR) signaling and expression undergo modifications in disorders such as addiction and depression, disease states also characterized by aberrant LHb neuronal firing (Bellone and Mameli, 2012; Hovelsø et al., 2012; Lecca et al., 2014). Group 1 mGluRs consist of mGluR1 and mGluR5 subtypes (Lüscher and Huber, 2010). Their activation modulates the strength of excitatory and inhibitory synapses through G_q/G_{11}-mediated calcium mobilization and activation of downstream effectors, including protein kinase C (PKC) (Lüscher and Huber, 2010; Page et al., 2001). Pre- and postsynaptic mechanisms underlie mGluR-dependent long-term plasticity, but its relevance for controlling neuronal activity remains poorly understood (Galante and Diana, 2004; Kammermeier et al., 2000; Mameli et al., 2007).

We combine electrophysiology in LHb-containing acute slices with pharmacology and find that activation of mGluR1 receptors, but not of mGluR5, triggers long-term depression of excitatory and inhibitory synaptic transmission (mGluR-eLTD and mGluR-iLTD, respectively). mGluR-eLTD and -iLTD induction requires postsynaptic PKC signaling, but their maintenance relies on divergent expression mechanisms. mGluR-eLTD occurs via a presynaptic cannabinoid 1 receptor (CB1-R)-dependent decrease in glutamate release. In contrast, mGluR-iLTD is independent of presynaptic changes. Instead, mGluR-iLTD is postsynaptically expressed and requires PKC targeting onto $GABA_A$-R β2-subunits and a reduction in $GABA_A$-R single-channel conductance. The functional relevance of mGluR activation in the LHb is represented by opposing effects on neuronal output. Indeed, in the LHb, the mGluR-driven modulation of synaptic responses and output firing correlate positively. These data unravel the distinct molecular mechanisms underlying mGluR control of synaptic strength and the subsequent regulation of LHb neuronal activity.

RESULTS

mGluRs Drive Long-Term Synaptic Depression in the LHb

To examine the presence of group I mGluRs, we microdissected the LHb of mice and employed RT-PCR, which revealed mGluR1 and mGluR5 expression (Figure 1A). Accordingly, bath application (3–5 min) of the mGluR1/5 agonist

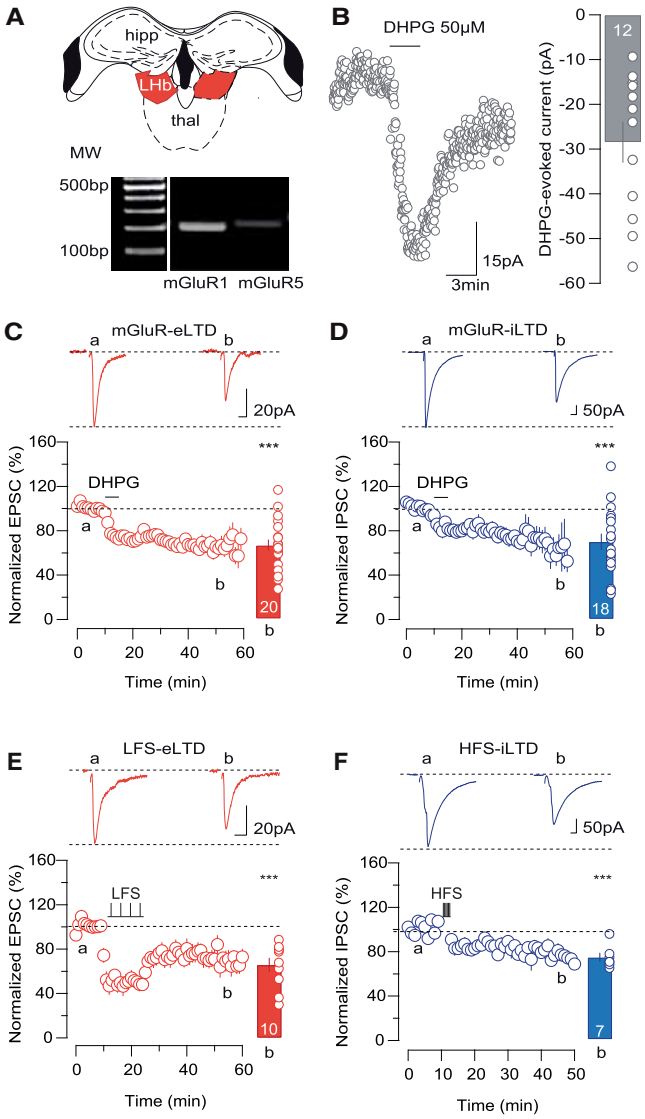

Figure 1. mGluR-eLTD and -iLTD in the LHb

(A) Schematic depicting the LHb microdissection (hipp, hippocampus; thal, thalamus) and mGluR1 and mGluR5 expression in the LHb. MW, molecular weight; bp: base pairs.

(B) Sample trace, bar graph, and scatterplot representing DHPG-evoked current (−28.5 ± 4.6 pA, 12 of 22 responding neurons).

(C) Sample traces representing EPSCs at baseline (a) and 20 min following DHPG (b). The timeline represents the DHPG effect (50 μM) on EPSCs. The bar graph and scatterplot show normalized averaged EPSCs ~40 min after DHPG (66.3 ± 5%, t_{19} = 6.306, ***p < 0.0001).

(D) The same as (C) but for IPSCs (69.9 ± 7.3%, t_{17} = 4.235, ***p < 0.0001).

(E) LFS-driven (1 Hz, 15 min) eLTD. The bar graph and scatterplot show normalized averaged EPSCs ~40 min after the protocol (65.8 ± 6.4%, t_9 = 5.3, ***p < 0.0001).

(F) HFS-driven (100 Hz, 1 s, at 0 mV) iLTD (top). The bar graph and scatterplot show normalized averaged IPSCs ~40 min after the protocol (74.2 ± 3.9%, t_6 = 7.086, ***p < 0.0001).

When not indicated, the timescale represents 5 ms. Error bars represent SEM. n indicates number of recorded neurons.

3,5-dihydroxyphenylglycine (DHPG, 50 μM) led to a transient inward current (Figure 1B; Gee et al., 2003). These data indicate the presence of functional postsynaptic group I mGluRs in LHb neurons.

To investigate whether mGluR activation modulates neurotransmission in the LHb, we tested the effect of DHPG application (5 min) on pharmacologically isolated AMPA receptor (AMPA-R)-mediated excitatory and $GABA_A$-R-mediated inhibitory postsynaptic currents (excitatory postsynaptic currents [EPSCs] and inhibitory postsynaptic currents [IPSCs], respectively). DHPG produced long-term depression of EPSCs and IPSCs (Figures 1C and 1D), termed eLTD and iLTD, respectively. mGluRs are activated by wide ranges of presynaptic activity (Lüscher and Huber 2010; Chevaleyre et al., 2006). Accordingly, we found that low-frequency stimulation (LFS) of presynaptic fibers (1 Hz) led to eLTD (Figure 1E). Instead, at inhibitory synapses, high-frequency stimulation (HFS) of presynaptic afferents (100 Hz at 0 mV) triggered iLTD (Figure 1F). Thus, mGluR activation and a distinct pattern of presynaptic activity in the LHb efficiently reduce excitatory and inhibitory synaptic transmission.

mGluR-eLTD and -iLTD Require mGluR1 and PKC Signaling

Group I mGluRs comprise mGluR1 and mGluR5 subtypes. To assess the induction requirement for mGluR- eLTD and -iLTD, we first exposed slices to either mGluR1 or mGluR5 antagonists (LY367385 or 3-2-methyl-4-thiazolyl-ethynyl-pyridine [MTEP], respectively). The mGluR1 antagonist LY367385 prevented DHPG eLTD/iLTD as well as LFS eLTD and HFS iLTD (Figures 2A and 2B; Figures S1A and S1B). Although the LFS protocol also reduced IPSCs, LY367385 failed to block this form of plasticity, indicating a different mechanism of induction (Figure S1C). Importantly, DHPG eLTD and iLTD remained intact in presence of the mGluR5 antagonist MTEP (Figures 2C and 2D).

Downstream of mGluRs, the G_q-coupled cascade leads to PKC activation, which targets a wide spectrum of synaptic proteins crucial for synaptic adaptations (Lüscher and Huber, 2010). To test PKC implication for mGluR-eLTD and -iLTD, we dialyzed neurons through a patch pipette with a pseudosubstrate peptide inhibitor of PKC, PKC[19-36] (Oliet et al., 1997). mGluR-eLTD and -iLTD were abolished in the presence of PKC[19-36] (Figures 2E and 2F). If PKC underlies mGluR-eLTD and -iLTD, we reasoned that its activation would occlude mGluR-driven synaptic plasticity. To test this, we bath-applied the PKC activator phorbol-12-myristate-13-acetate (PMA). When PMA successfully decreased EPSCs and IPSCs (seven of ten and five of six cells, respectively; Figures 2G and 2H), subsequent DHPG application failed to further reduce excitatory and inhibitory synaptic responses (Figures 2G and 2H). These data indicate that mGluR activation decreases excitatory and inhibitory synaptic transmission via a common mechanism requiring mGluR1-driven PKC signaling.

Presynaptic Expression Mechanism of eLTD in the LHb

Excitatory synapses in the LHb contain GluA2-lacking AMPA-Rs, as indicated by inwardly rectifying EPSCs (Maroteaux and Mameli, 2012). In brain structures such as the ventral tegmental

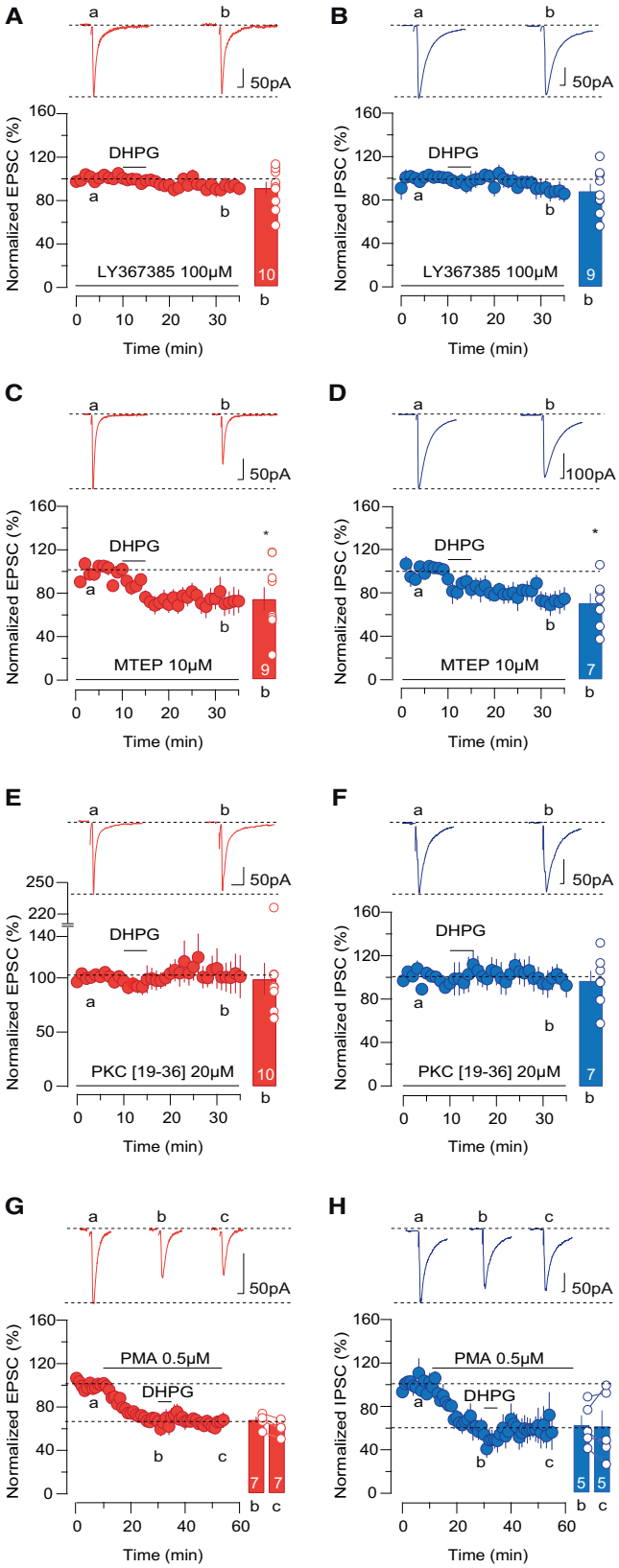

Figure 2. mGluR1 and PKC-Dependent Induction for eLTD and iLTD

(A) DHPG effect on EPSCs in the presence of the mGluR1 antagonist LY367385 (91.1 ± 5.6%, t_9 = 2.063, p > 0.05).

(B) The same as (A) but for IPSCs (88.7 ± 6.7%, t_8 = 1.680, p > 0.05).

(C) DHPG effect on EPSCs in the presence of the mGluR5 antagonist MTEP (74.5 ± 10.8%, t_8 = 2.377, *p < 0.05).

(D) The same as (C) but for IPSCs (71 ± 8.7%, t_6 = 3.425, *p < 0.05).

(E) DHPG effect on EPSCs during intracellular dialysis of PKC[19-36] (99.2 ± 14.8%, t_9 = 0.066, p > 0.5).

(F) The same as (E) but for IPSCs (98.1 ± 9.1%, t_6 = 0.088, p > 0.05).

(G) Effect of PMA on EPSCs (b, baseline versus PMA, 68.2 ± 2.4%, t_6 = 13.39, ***p < 0.0001) and subsequent occlusion of DHPG eLTD (c, PMA versus post-DHPG, 64.2 ± 5%, t_6 = 1.260, p > 0.05).

(H) The same as (G) but for IPSCs (b, baseline versus PMA, 62.7 ± 8.7%, t_4 = 4.285, *p < 0.05; c, PMA versus post-DHPG, 61.7 ± 14.4%, t_4 = 0.155, p > 0.05).

Error bars represent SEM. n indicates number of recorded neurons.

area, nucleus accumbens, and cerebellum, the presence of GluA2-lacking AMPA-Rs is a requirement for mGluRs to trigger postsynaptic LTD. This form of plasticity occurs via a switch from GluA2-lacking high-conductive to GluA2-containing low-conductive AMPA-Rs (Bellone and Lüscher, 2005; Kelly et al., 2009; McCutcheon et al., 2011). To test whether this scenario also applies to the LHb, we evoked EPSCs at different holding potentials (–60, 0, and +40 mV) before and after mGluR-eLTD (Figure 3A). EPSCs at baseline were inwardly rectifying, yielding a rectification index of >1, indicative of GluA2-lacking AMPA-R expression. DHPG reduced EPSC amplitude at negative and positive potentials, leaving the rectification index unaltered (Figure 3A). Thus, mGluR-eLTD in the LHb does not require postsynaptic modifications of AMPA-R subunit composition.

Aside from postsynaptic modifications, mGluRs can also trigger presynaptic long-term adaptations. To examine whether a decrease in presynaptic glutamate release underlies mGluR-eLTD, we monitored the paired-pulse ratio (PPR) of EPSCs before and after DHPG and LFS. Along with the reduced EPSC amplitude, DHPG application as well as the LFS produced a long-lasting increase in the PPR, indicating reduced glutamate release (Figure 3B; Figures S2A–S2C). In line with the mGluR1 and PKC requirements for mGluR-eLTD, the PPR remained unaltered after DHPG in the presence of the mGluR1 antagonist and PKC inhibitor but not in the presence of the mGluR5 blocker (Figure 3B). Interestingly, PMA-driven reduction in EPSCs occurred along with an increased PPR, which remained unaffected after subsequent DHPG application (Figure 3B). The different pharmacological agents did not alter the baseline PPR, suggesting the absence of drug-induced modifications in the probability of glutamate release (Figure 3B; black columns for all conditions). To corroborate our findings on the presynaptic mechanism underlying mGluR-eLTD, we examined quantal release by recording miniature EPSCs (mEPSCs). In the presence of tetrodotoxin, DHPG application led to a decrease in mEPSC frequency without significant changes in mEPSC amplitude (Figure 3C). This supports a scenario for a presynaptic expression of mGluR-eLTD. mGluR activation can trigger the release of endocannabinoids from postsynaptic neurons in several brain structures, including the striatum, hippocampus, and ventral tegmental area. mGluR-driven endocannabinoid mobilization acts retrogradely on presynaptic CB1-Rs,

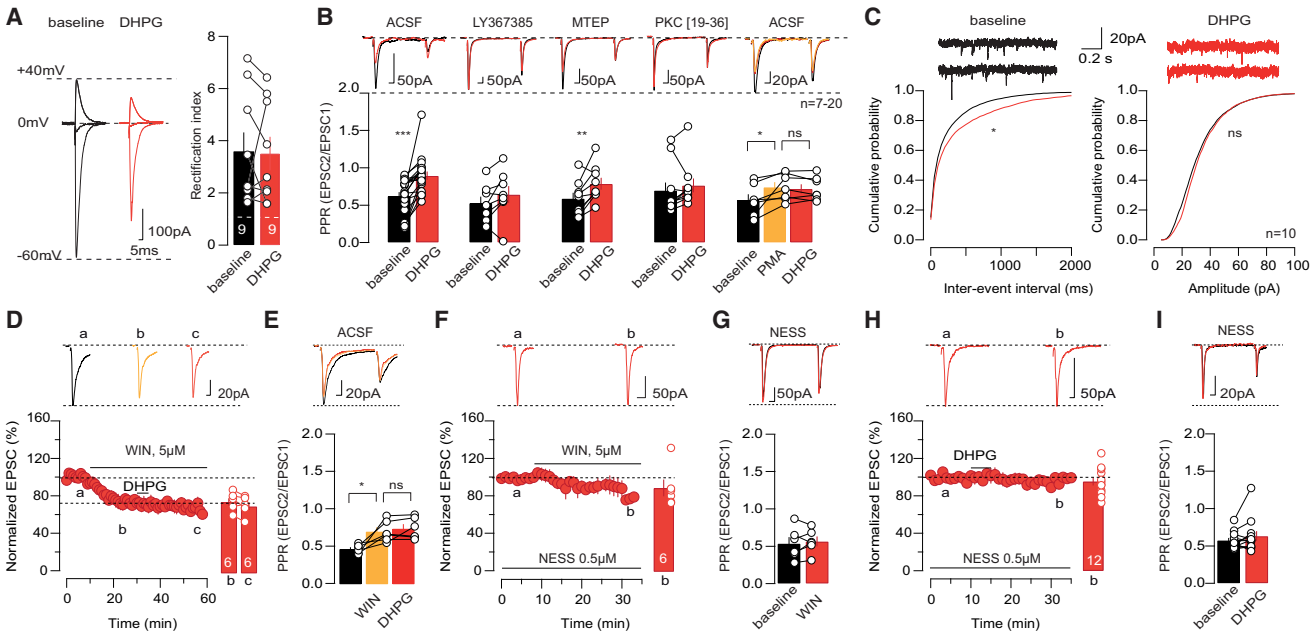

Figure 3. mGluR-eLTD Expression via CB1-R Activation

(A) Sample traces of AMPA-EPSCs at –60, 0, and +40 mV at baseline and after DHPG and average rectification index (baseline 3.6 ± 0.7 versus post-DHPG 3.5 ± 0.6, $t_8 = 0.192$, $p > 0.05$).

(B) PPR of EPSCs in artificial cerebrospinal fluid (ASCF; baseline 0.62 ± 0.05 versus post-DHPG 0.9 ± 0.05, $t_{19} = 4.963$, ***$p < 0.0001$); in the presence of LY367385 (baseline 0.53 ± 0.08 versus post-DHPG 0.64 ± 0.11, $t_7 = 1.860$, $p > 0.05$); of MTEP (baseline 0.59 ± 0.08 versus post-DHPG 0.79 ± 0.08, $t_8 = 3.432$, **$p < 0.01$); of PKC[19-36] in the recording pipette (baseline 0.7 ± 0.1 versus post-DHPG 0.76 ± 0.1, $t_9 = 1.214$, $p > 0.05$); after PMA and PMA + DHPG (baseline 0.57 ± 0.08 versus PMA 0.74 ± 0.07, $t_6 = 2.799$,*$p < 0.05$; PMA baseline versus PMA post-DHPG, $t_6 = 0.829$, $p > 0.05$). Shown are neurons represented in Figures 1 and 2. One-way ANOVA among all baseline PPR conditions: $F_{(9, 83)} = 0.485$, $p > 0.05$.

(C) Top: sample traces for mEPSCs. Cumulative probability plots show amplitudes and inter-event intervals for mEPSCs at baseline (black) and after DHPG (red). (mEPSC amplitude: baseline 30 ± 3.8 pA versus post-DHPG 32.1 ± 4.1 pA, KS test, $p > 0.05$; mEPSC frequency: baseline 3.8 ± 1.6 Hz versus post-DHPG 2.5 ± 1.1 Hz, KS test, *$p < 0.05$).

(D) Effect of WIN-55,212-2 on EPSCs (72.7 ± 3.8%, $t_5 = 7.246$, ***$p < 0.001$) and subsequent occlusion after DHPG application (68.5 ± 3.9%, $t_5 = 5.559$, $p > 0.05$).

(E) PPR of EPSCs after WIN application and subsequent DHPG application (baseline 0.45 ± 0.02, post-WIN 0.67 ± 0.05, post-DHPG 0.71 ± 0.06; baseline versus post-WIN, $t_5 = 3.411$, *$p < 0.05$; post-WIN versus post-DHPG, $t_5 = 1.004$, $p > 0.05$).

(F) The same as (D) but in the presence of NESS-0327 (90.79 ± 9.02%, $t_5 = 1.001$, $p > 0.05$).

(G) The same as (E) but in the presence of NESS-0327 (baseline 0.54 ± 0.09 versus post-WIN 0.57 ± 0.06, $t_5 = 0.672$ $p > 0.05$).

(H) Effect of DHPG on EPSCs in the presence of NESS-0327 (95.9 ± 4.3%, $t_{11} = 0.766$, $p > 0.05$).

(I) PPR after DHPG in the presence of NESS-0327 (baseline 0.58 ± 0.03 versus post-DHPG 0.63 ± 0.06, $t_{11} = 1.404$, $p > 0.05$).

Error bars represent SEM. n indicates number of recorded neurons.

negatively modulating neurotransmitter release (Heifets and Castillo, 2009). However, whether mGluRs trigger endocannabinoid signaling within the LHb is unknown. We first tested whether CB1-Rs are functionally expressed in the LHb. The CB1-R agonist WIN-55,212-2 reduced EPSC amplitude and increased the PPR (Figures 3D and 3E). This intervention occluded DHPG eLTD, suggesting that mGluR-eLTD expresses through CB1-R activation (Figures 3D and 3E). We pharmacologically confirmed that CB1-Rs are required for WIN-55,212-2-driven EPSC reduction because this was prevented by bath application of the CB1-R neutral antagonist NESS-0327 (Meye et al., 2013; Figures 3F and 3G). Consistent with the idea that CB1-Rs underlie the presynaptic expression of mGluR-eLTD, NESS-0327 also prevented mGluR-dependent plasticity and the concomitant increase in PPR (Figures 3H and 3I). This suggests that mGluR-eLTD requires a PKC-dependent and CB1-Rs-mediated reduction in presynaptic glutamate release.

Postsynaptic Mechanisms for mGluR-iLTD in the LHb

Because mGluR-driven endocannabinoid mobilization can also modulate GABA transmission (Chevaleyre et al., 2006), we questioned whether mGluR-iLTD requires a reduction in GABA release. We first examined the PPR of IPSCs before and after DHPG or HFS. mGluR-iLTD and HFS-iLTD occurred without PPR modifications, independent of the pharmacological intervention, suggesting the absence of presynaptic adaptations at inhibitory synapses (Figure 4A; Figures S2B and S2D). In line with this finding, mIPSC frequency remained unchanged, whereas mIPSCs amplitude decreased after DHPG application (Figure 4B). Moreover, NESS-0327 did not prevent the mGluR-dependent reduction in GABAergic transmission (Figure 4C). Together, these findings support that mGluR-iLTD is independent of endocannabinoid-driven presynaptic modifications. These data suggest instead a postsynaptic expression mechanism for mGluR-iLTD in contrast to the presynaptically expressed mGluR-eLTD.

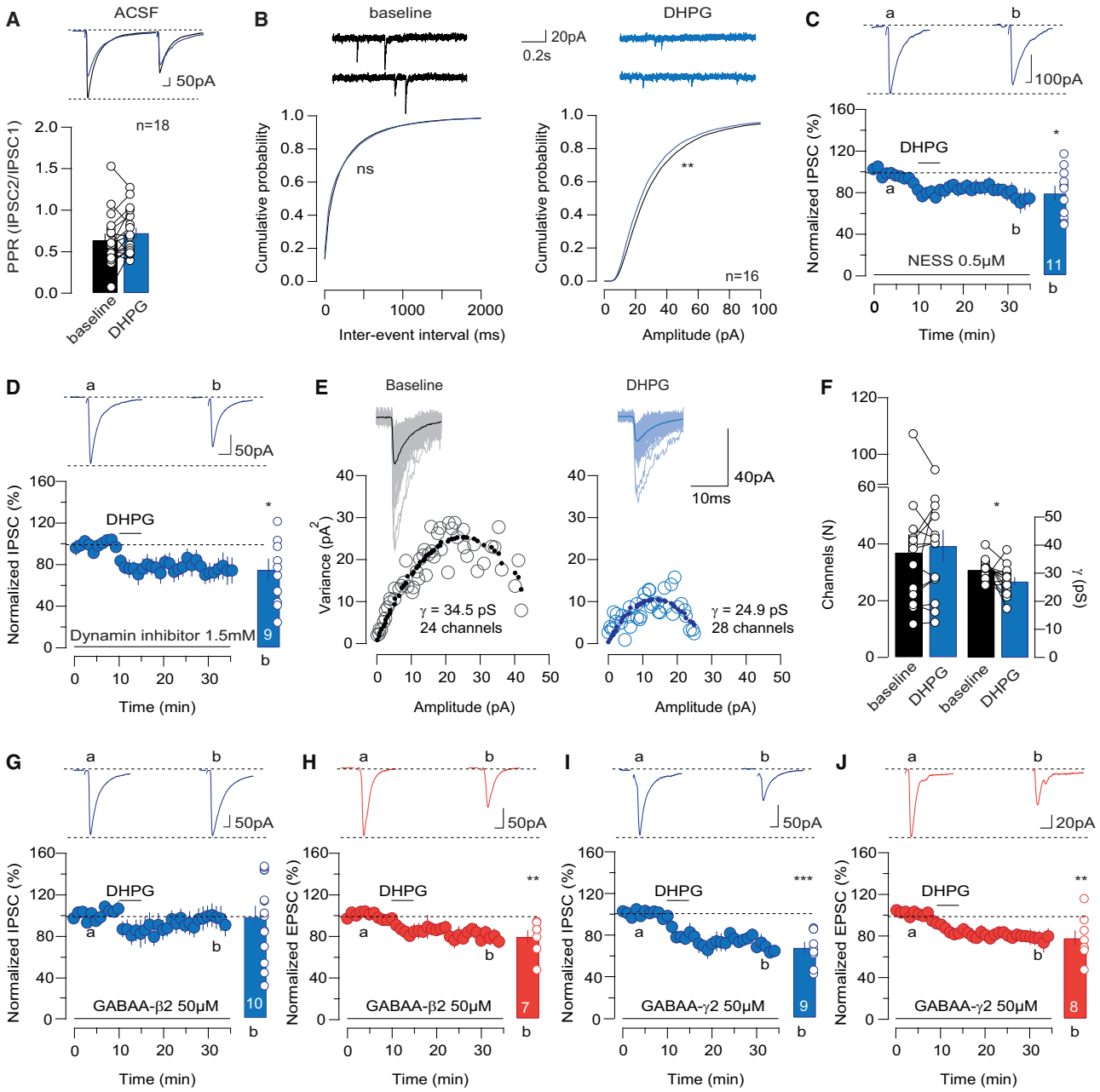

Figure 4. PKC Action on the $GABA_A$-Rs-β2 Subunit Underlies mGluR-iLTD

(A) PPR of IPSCs after DHPG (baseline 0.64 ± 0.07 versus post-DHPG 0.73 ± 0.06, t_{17} = 1.739, p > 0.05).

(B) Top: sample traces of mIPSCs. Cumulative probability plots show inter-event intervals and amplitudes for IPSCs at baseline (black) and after DHPG (blue) (mIPSC amplitude: baseline 41.3 ± 5.9 pA versus post-DHPG 39.2 ± 4.83 pA, KS test, **p < 0.01; mIPSC frequency: baseline 3.6 ± 1.09 Hz versus post-DHPG 3.45 ± 1.13 Hz, KS test, p > 0.05).

(C) Effect of DHPG on IPSCs in the presence of NESS-0327 (79.1 ± 7.06%, t_{10} = 2.621, *p < 0.05).

(D) DHPG effect on IPSCs in the presence of intracellular dynamin inhibitor (75.2 ± 10.2%, t_8 = 2.378, *p < 0.05).

(E) Example of peak-scaled NSFA of mIPSCs at baseline (black) and after DHPG (blue). Insets, overlay and average of analyzed traces.

(F) Pooled data for N and γ after NSFA (N: baseline 37 ± 6.3 versus post-DHPG 39.3 ± 5.6; t_{13} = 0.8, p > 0.05; γ: baseline 31.4 ± 1 versus post-DHPG 27.2 ± 1.4; t_{13} = 2.4, *p < 0.05).

(G) The same as (D) but in the presence of intracellular $GABA_A$-β2 peptide (97.7 ± 10.4%, t_{13} = 0.225, p > 0.05).

(H) The same as (G) but for EPSCs (78.8 ± 6.3%, t_6 = 3.488, *p < 0.05).

(I) The same as (G) but in the presence of intracellular $GABA_A$-γ2 peptide (67.7 ± 5.5%, t_8 = 6.141, ***p < 0.001).

(J) The same as (I) but for EPSCs (77.7 ± 7.4%, t_7 = 3.014, *p < 0.05).

Error bars represent SEM. n indicates number of recorded neurons.

Whether and how mGluR-PKC signaling modulates postsynaptic $GABA_A$-R function remains unknown. PKC can directly target $GABA_A$-Rs as well as auxiliary proteins modifying receptors' membrane expression and function (Kittler and Moss, 2003). For instance, PKC activation can increase $GABA_A$-R internalization via a dynamin-dependent mechanism (Herring et al., 2005). To examine whether mGluR-iLTD in the LHb requires $GABA_A$-R internalization, we dialyzed neurons with a membrane-impermeable dynamin inhibitor to prevent endocytosis. This intervention left mGluR-iLTD intact (Figure 4D), suggesting that $GABA_A$-R internalization is not required. To corroborate the absence of changes in the number of postsynaptic $GABA_A$-Rs during mGluR-iLTD, we employed peak-scaled non-stationary fluctuation analysis (NSFA) of mIPSCs (Maroteaux and Mameli, 2012; Nusser et al., 2001). Based on the stochastic closing of ion channels, this statistical method allows us to estimate the number of receptors opened (N) by neurotransmitter release as well as their single-channel conductance (γ). Plotting the decay variance as a function of the mean current amplitude for all recorded neurons yielded $\gamma_{GABA\text{-}A\text{-}R}$ values comparable to previous studies (31.4 ± 1 pS; Figures 4E and 4F; Nusser et al., 2001). DHPG decreased estimated $\gamma_{GABA\text{-}A\text{-}Rs}$ without altering estimated $N_{GABA\text{-}A\text{-}Rs}$ (Figures 4E and 4F). Together, this supports the absence of mGluR-driven $GABA_A$-R internalization. Conversely, a reduction in $\gamma_{GABA\text{-}A\text{-}R}$ suggests a decrease in $GABA_A$-R function, a modulation that may result from subunit-specific PKC-mediated phosphorylation (Kittler and Moss, 2003). Consistently, PKC-driven phosphorylation of specific serine residues on the $GABA_A$-R β1-3 and γ2 subunits reduces receptor function without altering the total receptor pool (Brandon et al., 2002a; Feng et al., 2001; Kittler and Moss, 2003). Given the reported expression of $GABA_A$-R β2 and γ2 subunits within the LHb (Hörtnagl et al., 2013), we predicted that the described mGluR-iLTD results from the direct PKC modulation of specific $GABA_A$-R subunits. To test this, we dialyzed dominant-negative peptides corresponding to the PKC-targeted sequences of $GABA_A$-R β2 or γ2 subunits (Brandon et al., 2000; Feng et al., 2001). The presence of the β2 peptide ($GABA_A$-β2) prevented mGluR-iLTD. In contrast, mGluR-eLTD and the concomitant PPR increase remained intact, ruling out non-specific actions of $GABA_A$-β2 dialysis (Figures 4G and 4H; Figures S2C and S2D). Intracellular infusion of the γ2 peptide ($GABA_A$-γ2) did not affect the expression of mGluR-iLTD or mGluR-eLTD (Figures 4I and 4J; Figures S2C and S2D). These data suggest that mGluRs trigger a PKC-dependent reduction in $GABA_A$-R conductance, likely occurring via phosphorylation of the β2 but not γ2 receptor subunits.

mGluRs Decide the Direction of LHb Neuronal Output

Opposed motivational states (i.e., reward and aversion) require bidirectional modification of LHb neuronal output, which can result in part from glutamatergic and GABAergic synaptic adaptations (Shabel et al., 2012; Stamatakis et al., 2013; Meye et al., 2015). What would be the functional repercussions of mGluR-eLTD and iLTD for LHb activity? To test the consequences of mGluR-LTD on LHb neuronal output, we recorded synaptically evoked postsynaptic potentials (PSPs) in current clamp mode. In the absence of synaptic blockers, PSPs result from a mixture of glutamatergic and GABAergic components and are therefore susceptible to mGluR-eLTD and -iLTD. We delivered trains of ten stimuli (20 Hz) and set the stimulation intensity so that ~50% of evoked PSPs would produce action potentials (APs) (Figure 5A). Ten minutes after DHPG washout, a time point where mGluR-eLTD and -iLTD are fully expressed, AP numbers either increased or decreased (>20% change in APs) in ~64% of neurons. Because of this dual modulation, DHPG did not, on average, modify the extent of evoked APs (Figure 5A). However, the bidirectional mGluR-driven change in neuronal activity may result from the expression of either mGluR-eLTD or -iLTD. Therefore, we examined whether the direction of LHb neuronal output after DHPG application correlates with mGluR-mediated modulation of PSPs. The area under individual PSPs (not including APs) was computed and averaged before and after DHPG to assess the PSPs potentiation or inhibition after mGluR activation. We predicted that the mGluR-mediated increase in PSPs would facilitate firing as a consequence of mGluR-iLTD. Conversely, predominant mGluReLTD would reduce the PSP area, decreasing neuronal output. In line with this scenario, the mGluR-driven change in PSP area positively correlated with the DHPG-driven modulation of AP number (Figures 5A and 5B). To determine the causality between mGluR-eLTD/iLTD and the firing adaptations, we prevented the expression mechanisms underlying mGluR-LTD at excitatory and inhibitory synapses. Concomitantly blocking CB1-R and PKC action on $GABA_A$-β2 receptors led to DHPG-driven modulation of LHb neuronal firing (>20% change in APs) in only 12.5% of recorded neurons. Under this condition, no correlation occurred between PSP area and firing after mGluR activation (Figures 5C and 5D). In contrast, independently preventing either mGluR-eLTD or -iLTD expression mechanisms revealed a marked bidirectional DHPG-induced modulation of evoked firing (Figures S3A and S3B). Furthermore, input resistance and AP properties did not change or correlate with DHPG-mediated firing changes (Figures S3C–S3H).

If the occurrence of mGluR-dependent plasticity differs at excitatory or inhibitory synapses from specific inputs, this would partly explain the predominant influence of either mGluR-eLTD or -iLTD on neuronal output. LHb neurons receive axons from the entopeduncular nucleus (EPN, EPN^{LHb}) that co-release glutamate and GABA (Shabel et al., 2012). This allows us to examine whether mGluR-LTD occurs in a neurotransmission-specific fashion at a precise synaptic input. As a proof of concept, we virally expressed channelrhodopsin-2 (ChR2) in the EPN. This led to $ChR2^+$ terminals within the lateral aspect of the LHb (Shabel et al., 2012; Meye et al., 2016; Figure S4A). DHPG bath application triggered a LTD of light-evoked EPN^{LHb} IPSCs, whereas light-evoked EPN^{LHb} EPSCs remained unaffected (Figures S4B and S4C). Together, these findings suggest that mGluRs in the LHb can control the direction of neuronal activity, likely via input-specific eLTD or iLTD.

DISCUSSION

Here we demonstrate that group I mGluRs decrease excitatory and inhibitory synaptic transmission in the LHb in a

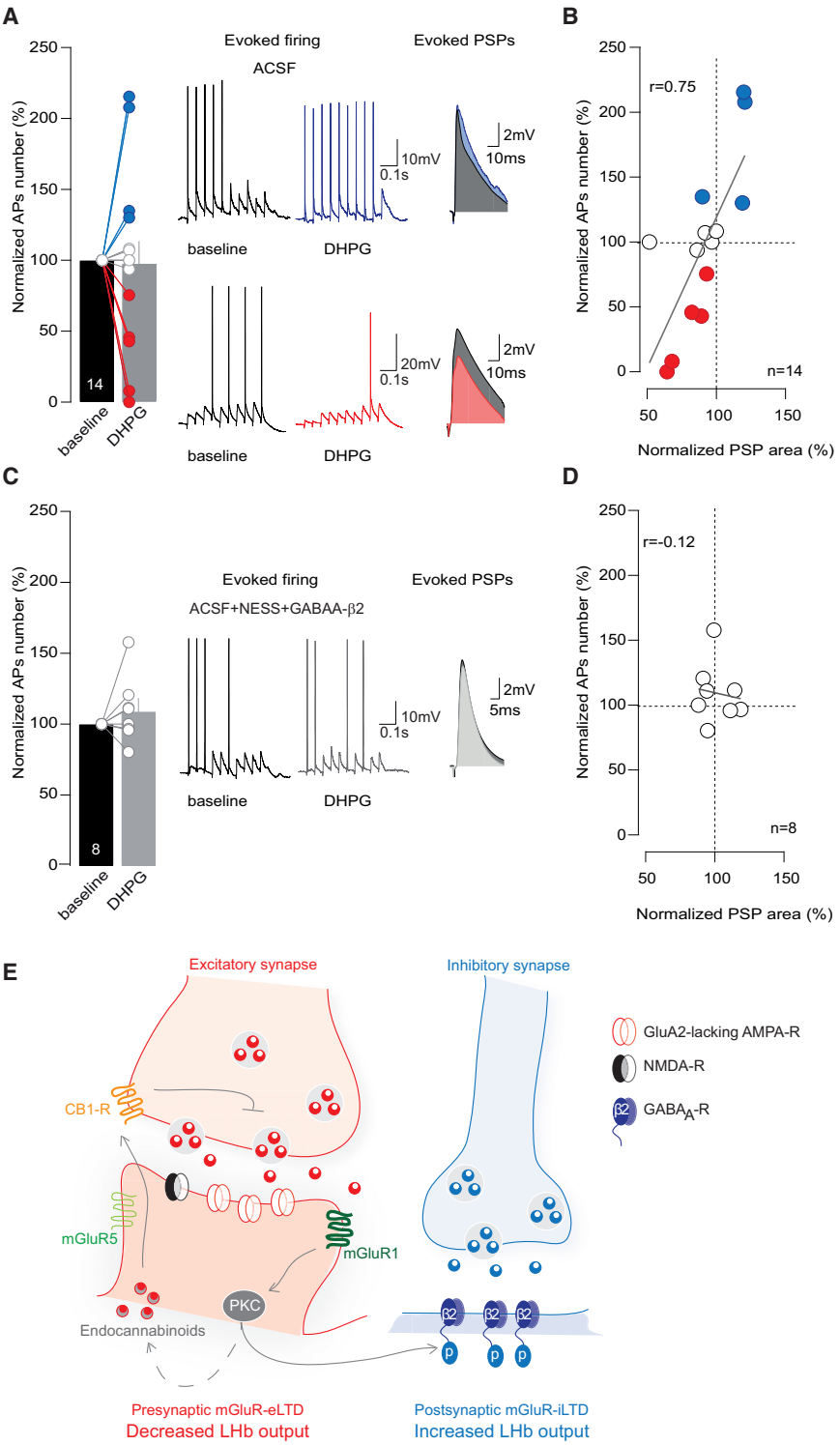

Figure 5. mGluR-Dependent Bidirectional Control of LHb Neuronal Output

(A) DHPG effect on synaptically evoked AP numbers in ACSF (97.7 ± 19.6; $t_{13} = 0.13$, $p > 0.05$). 4 of 14 recorded neurons increased in firing (blue), and 5 of 14 decreased in firing (red) following DHPG. Sample traces indicate the bidirectional nature (blue increased firing, red decreased firing) of mGluR activation. Shown are superimposed EPSPs at baseline (black) and after DHPG (blue, increased firing; red, decreased firing).

(B) Correlation between normalized mGluR-driven firing and normalized PSP area (Pearson correlation, $r = 0.75$, $^{**}p < 0.01$).

(C) The same as (A) but in the presence of NESS-0327 and $GABA_A$-β2 peptide in the internal solution (109.2 ± 8.2, $t_7 = 1.12$, $p > 0.05$). Black and gray traces represent before and after DHPG.

(D) The same as (B) but in the presence of NESS-0327 in the ACSF and $GABA_A$-β2 peptide in the internal solution (Pearson correlation, $r = -0.12$, $p > 0.05$). Fisher r-to-z transformation for (B) versus (D) correlations yielded a Z score of 2.03. $^{*}p < 0.05$.

(E) Schematic indicating the induction and expression mechanisms for mGluR-eLTD and -iLTD and their relative contribution to LHb neuronal output.

Error bars represent SEM. n indicates number of recorded neurons.

PKC-dependent manner. On one hand, mGluR1-driven PKC activation in LHb represents a common process at excitatory and inhibitory synapses. On the other hand, mGluR1 signaling diverges at the level of PKC, targeting distinct substrates but leading to decreased glutamatergic and GABAergic neurotransmission. mGluR-eLTD and -iLTD modulate PSPs to decide the direction of LHb neuronal output. Our data support a scenario in which mGluRs modulate glutamatergic and GABAergic synapses in the LHb, contributing to adaptations in their computational properties potentially relevant for motivational states.

Notably, excitatory synapses in the LHb contain rectifying GluA2-lacking AMPA-Rs (Maroteaux and Mameli, 2012). A recent hypothesis posits that GluA2-lacking AMPA-R expression represents a predictive factor for a postsynaptic mGluR1-LTD requiring a subunit composition switch (Loweth et al., 2013). However, mGluR1 activation in the LHb reduces excitatory synaptic transmission while leaving the GluA2-lacking AMPA-R current-voltage relationship unchanged. This unaffected AMPA-Rs rectification may result from LHb-specific interactions between receptors and scaffolding proteins or, alternatively, from unidentified AMPA-Rs subtypes that would need to be further investigated.

In contrast, mGluR1s in the LHb act through postsynaptic PKC signaling to reduce glutamate release via CB1-R activation. Together with evidence indicating that LHb contains the endocannabinoid-synthesizing enzyme diacylglicerol lipase (Suárez et al., 2011), our data support functional endocannabinoid

signaling within the LHb. mGluR-driven endocannabinoid LTD is also observed at inhibitory synapses (Chevaleyre et al., 2006); however, this does not hold true in the LHb. Indeed, mGluR-iLTD is independent of presynaptic modifications and remains intact in the presence of CB1-R blockers. Although mGluR-iLTD does not require CB1-Rs, other G_q protein-coupled receptors (GPCRs) may mobilize endocannabinoids to drive iLTD. Future studies need to address whether CB1-R activation modifies GABA transmission or whether other GPCRs mediate endocannabinoid-dependent iLTD in the LHb.

Although PKC mediates the presynaptic expression of mGluR-eLTD, it reduces GABA transmission through a postsynaptic mechanism. Importantly, postsynaptic PKC signaling controls the strength of inhibitory neurotransmission (Kittler and Moss, 2003). For instance, PKC can induce rapid internalization of $GABA_A$-Rs through its actions on specific serine residues (Chapell et al., 1998; Herring et al., 2005). However, mGluR-iLTD in the LHb is independent of dynamin-mediated endocytosis and does not involve a reduction in the number of activated receptors. Instead, mGluRs promote a reduction in $GABA_A$-R single-channel conductance. This modification in $GABA_A$-R function may result from alterations in subunit composition, scaffolding proteins, and phosphorylation events (Kittler and Moss, 2003). Indeed, PKC reduces $GABA_A$-R function, but not receptor expression, via phosphorylation of key residues on the $GABA_A$-R β and γ subunits (Brandon et al., 2000, 2002b; Feng et al., 2001). We report that PKC action on $GABA_A$-R β2-subunits, but not on γ2 subunits, is crucial for mGluR-iLTD in the LHb. Interestingly, different subtypes of G_q-PCRs other than group I mGluRs (i.e., muscarinic acetylcholine and serotonin receptors) also reduce $GABA_A$-R function by PKC targeting of $GABA_A$-R β1 and γ2 subunits (Feng et al., 2001; Brandon et al., 2002a). This evidence therefore raises the possibility that different classes of G_q-PCRs across the CNS may reduce synaptic inhibition via PKC phosphorylation of specific $GABA_A$-R subunits (i.e., β2, γ2, β1) (Brandon et al., 2002b; Feng et al., 2001; Kittler and Moss, 2003).

mGluR-eLTD and -iLTD are widespread across many synapses (Chevaleyre et al., 2006), but their functional repercussions on neuronal output remain elusive. mGluR1 can affect potassium and calcium conductances, crucial for neuronal activity (Anwyl, 1999). However, the reported absence of changes in input resistance and AP properties suggests that mGluR-driven modulation of neuronal activity likely arises from synaptic adaptations. The mGluR-dependent potentiation and inhibition of PSPs indeed predicts the direction of neuronal output after mGluR activation. Moreover, precluding mGluR-eLTD and -iLTD concomitantly or independently unravels the causality between synaptic plasticity and mGluR-dependent control of LHb neuronal firing. This result also suggests that mGluR-eLTD and -iLTD likely do not occur simultaneously at the same locus and with the same extent. Instead, one predominates over the other, to drive, in different neurons, opposite neuronal output changes. mGluR-eLTD and -iLTD may occur together with similar magnitude but on distinct postsynaptic sites or even distinct LHb neuronal populations. In both cases, mGluR plasticity would ultimately lead to a bidirectional modulation of LHb global activity. These scenarios may rely, to some degree, on circuit specificity. The observation that the EPN^{LHb} GABAergic but not glutamatergic component is affected by mGluRs strongly suggests that, in the LHb, mGluR1 modulation may occur in a neurotransmission- and input-specific fashion. This is in in line with our data indicating that different patterns of activity trigger either mGluR-eLTD or -iLTD, and it is further supported by findings describing that input/output-specific plasticity controls LHb output firing (Shabel et al., 2014; Meye et al., 2016). In conclusion, these findings identify how mGluR1 signaling in the LHb diverges at the level of PKC, leading to reduced presynaptic glutamate release and postsynaptic $GABA_A$-R function. Based on our results, we speculate that mGluR-LTD in the LHb can decide the direction of neuronal activity, potentially influencing opposing motivational states.

EXPERIMENTAL PROCEDURES

Animals

C57Bl/6J male mice (~30 days old) were used in accordance with the guidelines of the French Agriculture and Forestry Ministry for handling animals, and protocols were validated by the Darwin#5 ethical committee of the University Pierre et Marie Curie. Mice were anesthetized (i.p.) with ketamine (150 mg/kg)/xylazine (100 mg/kg) (Sigma-Aldrich) prior to brain slice preparation or viral injections (Supplemental Experimental Procedures).

In Vitro Electrophysiology

Sagittal slices (250 μm) containing the LHb were prepared, and recordings were performed as described previously (Maroteaux and Mameli, 2012). For voltage clamp experiments, the internal solution contained 130 mM CsCl, 4 mM NaCl, 2 mM $MgCl_2$, 1.1 mM EGTA, 5 mM HEPES, 2 mM Na_2ATP, 0.6 mM Na_3GTP, 5 mM Na^+ creatine phosphate, 2 mM QX-314, and 0.1 mM spermine ; (pH 7.3), osmolarity ~300 mOsm. The holding potential was –50 mV. Synaptic currents were evoked through a glass pipette placed in the stria medullaris (60 μs at 0.1 Hz). The PPR was monitored (2 pulses, 20 Hz) and calculated as follows: $EPSC_2/EPSC_1$. mGluRs were activated by DHPG (50 μM) in the presence of 2,3-dihydroxy-6-nitro-7-sulfamoyl-benzo[f]quinoxaline-2,3-dione (NBQX; 10 μM) and D-(2*R*)-amino-5-phosphonovaleric acid; (2*R*)-amino-5-phosphonopentanoate (D-APV; 50–100 μM) or picrotoxin (100 μM). An LFS protocol (1 Hz, 15 min) or an HFS protocol (100 Hz at 0 mV for 1 s, 5 times every 10 s) was used for synaptic activation of mGluRs. The rectification index of AMPA-EPSCs was calculated as follows: $((I_{EPSC(-60)}/I_{EPSC(+40)})/1.5)$. Experiments assessing the postsynaptic effects of DHPG (voltage clamp) and output firing (current clamp) were performed with internal solution containing 140 mM KGluconate, 5 mM KCl, 10 mM HEPES, 0.2 mM EGTA, 2 mM $MgCl_2$, 4 mM Na_2ATP, 0.3 mM Na_3GTP, and 10 mM creatine phosphate; (pH 7.3), osmolarity ~300 mOsm. The input resistance was calculated via a 50-ms hyperpolarizing current (I = 20 pA) step (Ri = resting membrane potential [RMP]/I).

Non-stationary Fluctuation Analysis

A peak-scaled non-stationary fluctuation analysis was made from mIPSCs (Synaptosoft; Supplemental Experimental Procedures).

Drugs and Peptides

Drugs were obtained from Abcam, Tocris, Hello Bio, or Latoxan and dissolved in water. Tetrodotoxin (TTX) was dissolved in citric acid (1%); picrotoxin, NESS-0327, WIN-55,212-2, and PMA in DMSO; and LY367385 in NaOH 10%. For PMA experiments, only cells responding to drug application were included in the analysis. Peptides used in the study were custom-made (GeneScript) or obtained from Tocris (Supplemental Experimental Procedures) and, when indicated, included in the internal solution.

Analysis

Analysis was performed using IGOR-6 (Wavemetrics) and MiniAnalysis (Synaptosoft). Kolmogorov-Smirnov (KS) test, Student's t test, or ANOVA were used throughout the study. n in the figures indicates number of recorded

neurons. All data are expressed as mean ± SEM. Significance was set at alpha = 0.05 using paired t test.

SUPPLEMENTAL INFORMATION

Supplemental Information includes Supplemental Experimental Procedures and four figures and can be found with this article online at http://dx.doi.org/10.1016/j.celrep.2016.07.064.

AUTHOR CONTRIBUTIONS

K.V. and M.M. designed and performed the experiments, analyzed the data, and wrote the paper.

ACKNOWLEDGMENTS

We thank M. Carta, V. Chevaleyre, C. Bellone, N. Gervasi, and the Poncer-Levi and M.M. laboratory for helpful discussions and comments. We thank I. Moutkine for help with PCR experiments. This work was supported by Inserm ATIP-AVENIR, the City of Paris, and the European Research Council (ERC) under the European Union's Seventh Framework Program (FP7/2007-2013)/ERC grant agreement number 335333 SalienSy (to M.M.). K.V. is supported by a Ph.D. fellowship from the doctoral school ED3C Paris.

Received: December 14, 2015
Revised: June 27, 2016
Accepted: July 25, 2016
Published: August 18, 2016

REFERENCES

Anwyl, R. (1999). Metabotropic glutamate receptors: electrophysiological properties and role in plasticity. Brain Res. Brain Res. Rev. *29*, 83–120.

Bellone, C., and Lüscher, C. (2005). mGluRs induce a long-term depression in the ventral tegmental area that involves a switch of the subunit composition of AMPA receptors. Eur. J. Neurosci. *21*, 1280–1288.

Bellone, C., and Mameli, M. (2012). mGluR-Dependent Synaptic Plasticity in Drug-Seeking. Front. Pharmacol. *3*, 159.

Brandon, N.J., Delmas, P., Kittler, J.T., McDonald, B.J., Sieghart, W., Brown, D.A., Smart, T.G., and Moss, S.J. (2000). GABAA receptor phosphorylation and functional modulation in cortical neurons by a protein kinase C-dependent pathway. J. Biol. Chem. *275*, 38856–38862.

Brandon, N., Jovanovic, J., and Moss, S. (2002a). Multiple roles of protein kinases in the modulation of gamma-aminobutyric acid(A) receptor function and cell surface expression. Pharmacol. Ther. *94*, 113–122.

Brandon, N.J., Jovanovic, J.N., Smart, T.G., and Moss, S.J. (2002b). Receptor for activated C kinase-1 facilitates protein kinase C-dependent phosphorylation and functional modulation of GABA(A) receptors with the activation of G-protein-coupled receptors. J. Neurosci. *22*, 6353–6361.

Chapell, R., Bueno, O.F., Alvarez-Hernandez, X., Robinson, L.C., and Leidenheimer, N.J. (1998). Activation of protein kinase C induces gamma-aminobutyric acid type A receptor internalization in Xenopus oocytes. J. Biol. Chem. *273*, 32595–32601.

Chevaleyre, V., Takahashi, K.A., and Castillo, P.E. (2006). Endocannabinoid-mediated synaptic plasticity in the CNS. Annu. Rev. Neurosci. *29*, 37–76.

Feng, J., Cai, X., Zhao, J., and Yan, Z. (2001). Serotonin receptors modulate GABA(A) receptor channels through activation of anchored protein kinase C in prefrontal cortical neurons. J. Neurosci. *21*, 6502–6511.

Galante, M., and Diana, M.A. (2004). Group I metabotropic glutamate receptors inhibit GABA release at interneuron-Purkinje cell synapses through endocannabinoid production. J. Neurosci. *24*, 4865–4874.

Gee, C.E., Benquet, P., and Gerber, U. (2003). Group I metabotropic glutamate receptors activate a calcium-sensitive transient receptor potential-like conductance in rat hippocampus. J. Physiol. *546*, 655–664.

Heifets, B.D., and Castillo, P.E. (2009). Endocannabinoid signaling and long-term synaptic plasticity. Annu. Rev. Physiol. *71*, 283–306.

Herring, D., Huang, R., Singh, M., Dillon, G.H., and Leidenheimer, N.J. (2005). PKC modulation of GABAA receptor endocytosis and function is inhibited by mutation of a dileucine motif within the receptor beta 2 subunit. Neuropharmacology *48*, 181–194.

Hörtnagl, H., Tasan, R.O., Wieselthaler, A., Kirchmair, E., Sieghart, W., and Sperk, G. (2013). Patterns of mRNA and protein expression for 12 GABAA receptor subunits in the mouse brain. Neuroscience *236*, 345–372.

Hovelsø, N., Sotty, F., Montezinho, L.P., Pinheiro, P.S., Herrik, K.F., and Mørk, A. (2012). Therapeutic potential of metabotropic glutamate receptor modulators. Curr. Neuropharmacol. *10*, 12–48.

Kammermeier, P.J., Xiao, B., Tu, J.C., Worley, P.F., and Ikeda, S.R. (2000). Homer proteins regulate coupling of group I metabotropic glutamate receptors to N-type calcium and M-type potassium channels. J. Neurosci. *20*, 7238–7245.

Kelly, L., Farrant, M., and Cull-Candy, S.G. (2009). Synaptic mGluR activation drives plasticity of calcium-permeable AMPA receptors. Nat. Neurosci. *12*, 593–601.

Kittler, J.T., and Moss, S.J. (2003). Modulation of GABAA receptor activity by phosphorylation and receptor trafficking: implications for the efficacy of synaptic inhibition. Curr. Opin. Neurobiol. *13*, 341–347.

Lecca, S., Meye, F.J., and Mameli, M. (2014). The lateral habenula in addiction and depression: an anatomical, synaptic and behavioral overview. Eur. J. Neurosci. *39*, 1170–1178.

Lecca, S., Pelosi, A., Tchenio, A., Moutkine, I., Lujan, R., Hervé, D., and Mameli, M. (2016). Rescue of GABAB and GIRK function in the lateral habenula by protein phosphatase 2A inhibition ameliorates depression-like phenotypes in mice. Nat. Med. *22*, 254–261.

Loweth, J.A., Tseng, K.Y., and Wolf, M.E. (2013). Using metabotropic glutamate receptors to modulate cocaine's synaptic and behavioral effects: mGluR1 finds a niche. Curr. Opin. Neurobiol. *23*, 500–506.

Lüscher, C., and Huber, K.M. (2010). Group 1 mGluR-dependent synaptic long-term depression: mechanisms and implications for circuitry and disease. Neuron *65*, 445–459.

Mameli, M., Balland, B., Luján, R., and Lüscher, C. (2007). Rapid synthesis and synaptic insertion of GluR2 for mGluR-LTD in the ventral tegmental area. Science *317*, 530–533.

Maroteaux, M., and Mameli, M. (2012). Cocaine evokes projection-specific synaptic plasticity of lateral habenula neurons. J. Neurosci. *32*, 12641–12646.

McCutcheon, J.E., Loweth, J.A., Ford, K.A., Marinelli, M., Wolf, M.E., and Tseng, K.Y. (2011). Group I mGluR activation reverses cocaine-induced accumulation of calcium-permeable AMPA receptors in nucleus accumbens synapses via a protein kinase C-dependent mechanism. J. Neurosci. *31*, 14536–14541.

Meye, F.J., Trezza, V., Vanderschuren, L.J., Ramakers, G.M., and Adan, R.A. (2013). Neutral antagonism at the cannabinoid 1 receptor: a safer treatment for obesity. Mol. Psychiatry *18*, 1294–1301.

Meye, F.J., Valentinova, K., Lecca, S., Marion-Poll, L., Maroteaux, M.J., Musardo, S., Moutkine, I., Gardoni, F., Huganir, R.L., Georges, F., and Mameli, M. (2015). Cocaine-evoked negative symptoms require AMPA receptor trafficking in the lateral habenula. Nat. Neurosci. *18*, 376–378.

Meye, F.J., Soiza-Reilly, M., Smit, T., Diana, M.A., Schwarz, M.K., and Mameli, M. (2016). Shifted pallidal co-release of GABA and glutamate in habenula drives cocaine withdrawal and relapse. Nat. Neurosci. *19*, 1019–1024.

Nusser, Z., Naylor, D., and Mody, I. (2001). Synapse-specific contribution of the variation of transmitter concentration to the decay of inhibitory postsynaptic currents. Biophys. J. *80*, 1251–1261.

Oliet, S.H., Malenka, R.C., and Nicoll, R.A. (1997). Two distinct forms of long-term depression coexist in CA1 hippocampal pyramidal cells. Neuron *18*, 969–982.

Page, G., Peeters, M., Najimi, M., Maloteaux, J.M., and Hermans, E. (2001). Modulation of the neuronal dopamine transporter activity by the metabotropic

glutamate receptor mGluR5 in rat striatal synaptosomes through phosphorylation mediated processes. J. Neurochem. *76*, 1282–1290.

Shabel, S.J., Proulx, C.D., Trias, A., Murphy, R.T., and Malinow, R. (2012). Input to the lateral habenula from the basal ganglia is excitatory, aversive, and suppressed by serotonin. Neuron *74*, 475–481.

Shabel, S.J., Proulx, C.D., Piriz, J., and Malinow, R. (2014). Mood regulation. GABA/glutamate co-release controls habenula output and is modified by antidepressant treatment. Science *345*, 1494–1498.

Stamatakis, A.M., Jennings, J.H., Ung, R.L., Blair, G.A., Weinberg, R.J., Neve, R.L., Boyce, F., Mattis, J., Ramakrishnan, C., Deisseroth, K., and Stuber, G.D. (2013). A unique population of ventral tegmental area neurons inhibits the lateral habenula to promote reward. Neuron *80*, 1039–1053.

Suárez, J., Ortíz, O., Puente, N., Bermúdez-Silva, F.J., Blanco, E., Fernández-Llebrez, P., Grandes, P., de Fonseca, F.R., and Moratalla, R. (2011). Distribution of diacylglycerol lipase alpha, an endocannabinoid synthesizing enzyme, in the rat forebrain. Neuroscience *192*, 112–131.